Use of COMSOL Multiphysics for Automated Electrostatic MEMS Sensor Design

Jill C. Blecke[1*] and Gordon G. Parker[1]
[1]Michigan Technological University
*Corresponding author: jcblecke@mtu.edu   1400 Townsend Dr.
R.L.Smith Bldg.
Houghton, MI 49931

Abstract: An optimization-based automated design tool using COMSOL Multiphysics and genetic algorithms was developed for design of a MEMS sensor. The discretized design variables included material distribution, electrode placement, actuation voltage and miscellaneous geometric dimensions. The fitness function aimed to increase the average sensed change in capacitance for a given change in density. The model makes use of three COMSOL applications – 3D Solid Stress-Strain with Squeezed Film Damping (SMSLD plus MMFD), Deformed Mesh (ALE) and Electrostatics (EMES). For a sample population of 100 members, after 15 generations, the fitness value was reduced by a factor of 10.

Keywords: MEMS resonant mass sensor, genetic algorithm optimization

1. Introduction

This paper highlights the development of an automated design tool to improve the performance of MEMS sensors using COMSOL Multiphysics and genetic algorithms. To demonstrate the tool, the design for a MEMS resonant mass sensor is described. The sensor is an electrostatically actuated, fixed-free microcantilever with capacitive position sensing capabilities. The sensor has a polymer coating to which airborne contaminants attach, causing a mass change. The objective of the tool is to assign a combination of sensor dimensions, material and electrodes such that the largest average change in capacitance is sensed for an accumulated change in mass.

Section 2 will introduce the basic sensor design and the configuration of the design variables. The optimization based genetic algorithm design process will be described in Section 3. Section 4 details the COMSOL models used to evaluate fitness values. Finally, the results of a sample MEMS sensor design will be shown in Section 5.

2. Device Configuration

The genetic algorithm based design tool was applied to a MEMS resonant mass sensor. The sensor is composed of a fixed-free micro-cantilever beam fabricated from poly-silicon. The device uses separate electrodes for electrostatic actuation and capacitive sensing. A mass change to the device causes a shift in the frequency response of the sensor.

Each configuration was defined discretely. The physical design space was divided into grid-like regions. A single bit determined if a region had material and a second bit determined if that region contained sensing or actuation electrode. An additional set of bits described the magnitude of the applied voltage, the thickness of the beam and the size of the initial gap between electrodes. A sample configuration is detailed in Figure 1.
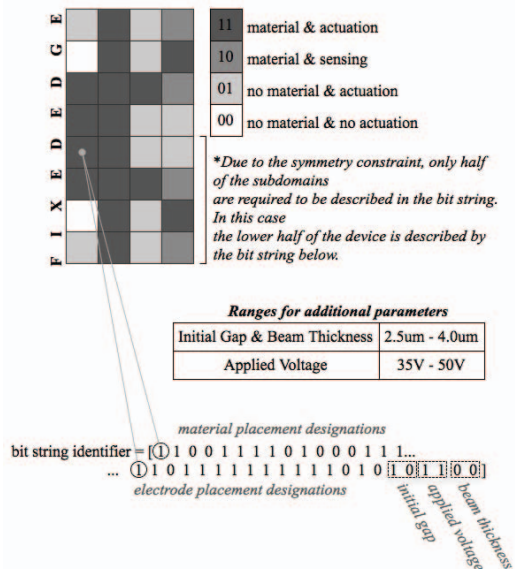

Figure 1: Sample configuration of a MEMS resonant mass sensor using the automated design tool.

3. Genetic Algorithm Based Design

Genetic algorithm optimization is an evolutionary based design method capable of searching a defined design space [1]. It is well suited for the discrete optimization problem presented in this paper. The numerical solution to a genetic algorithm design problem is defined by the number of members in the population, number of generations and the fitness function to be minimized. The diagram in Figure 2 describes the design process.

Step 1 was to generate an initial population. Then each member of the population was evaluated and ranked according to the fitness value in step 2. At step 3, a generation check was performed. If the current generation was not the final generation, step 4 was to create the population of the next generation and cycle back to step 2. A generation was created by a combination of 3 methods – elite members, crossover and mutation. In elite members, the highest ranked configurations automatically survived to the next generation. Crossover combined two members to form a new member for the next generation. Mutation utilized a small probability for adaption of a current member in its formation of a new member. After evaluation of the final generation the automation design loop was halted. The output solution was the configuration with the lowest fitness value in the final generation.

4. Use of COMSOL Multiphysics

The evaluation of each configuration relied on finite element analyses using COMSOL. This section will detail those models and the fitness calculation. Section 4.1 will discuss the construction of the geometry. Section 4.2-4.4 will describe the three COMSOL models used in the fitness calculation. Finally, the fitness computation will be detailed in Section 4.5.

4.1 Geometry Construction

In order to implement the boundary conditions in the applications for each individual region of the design space, the geometry was created in pieces and combined, preserving the original boundaries. A solid 3D block was drawn to represent each region of the beam and is referred to in the remaining sections of the paper
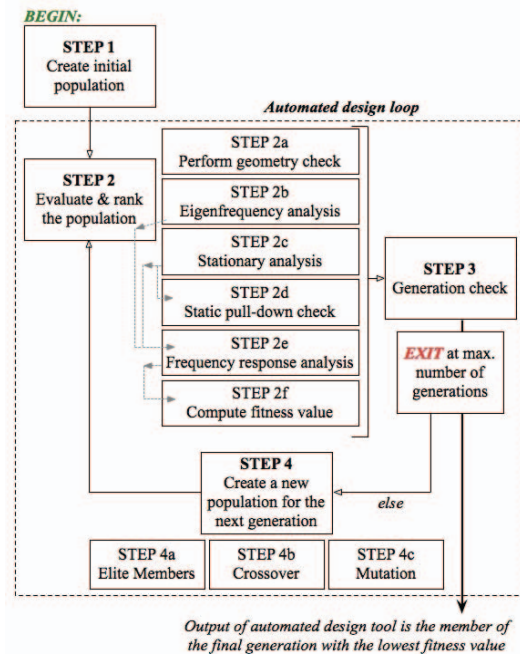

Figure 2: Process flow of the automated design tool integrating the use of COMSOL & genetic algorithms

as a "beam subdomain." A second 3D block was drawn to represent the air gap beneath the "beam subdomain" and is referred to in the remaining sections of the paper as an "electrostatic subdomain." Finally, a larger block was drawn to encompass the entire beam and the air gap to allow for evaluation and visualization of the electrostatic field around the device. The total number of regions in the geometry was dependent upon the number of rows and columns specified. The length and width of each region was specified at the beginning of the program and remained consistent throughout the design process. In this example, each region was assumed to be 10 μm long and 10 μm wide.

In the random member generation of the genetic algorithm design tool it is possible to create infeasible geometry configurations. For example, cantilever beams with no material elements on the fixed-end of the beam or floating portions of material are considered invalid designs. Examples of valid and invalid configurations are illustrated in Figure 3.

To avoid invalid geometries in the first population, an initial population function was created in MATLAB that only generated configurations with connected geometries.
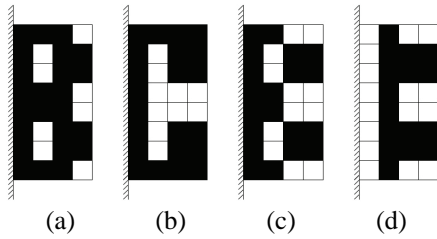
Figure 3: Examples of valid geometries (a)-(b) and invalid geometries (c)-(d) where shaded regions represent material and white regions represent void

However, invalid geometries could still be generated in the crossover and mutation processes. A geometry check was performed for each configuration before fitness evaluation. If a particular geometry was found to be invalid, it was discarded and replaced by a new geometry created by the initial population function.

4.2 Model 1: Eigenfrequency Analysis

The fitness evaluation investigates the change in natural frequency of the sensor after a mass change. Thus, the natural frequency of the device must be computed before and after the mass accumulation using an eigenfrequency analysis in the SMSLD application (Step 2b in Figure 2). The mass change of the device was modeled as a 0.1% increase in density. A function was created in MATLAB to compute the indices for proper assignment of subdomain and boundary properties.

Table I summarizes the subdomain settings used in this model. Beam subdomains with material were active in this application and assigned poly-silicon material properties. The remaining subdomains were inactive for this analysis.

Table I: Subdomain settings for the natural frequency computation of the device before and after mass accumulation on the sensor

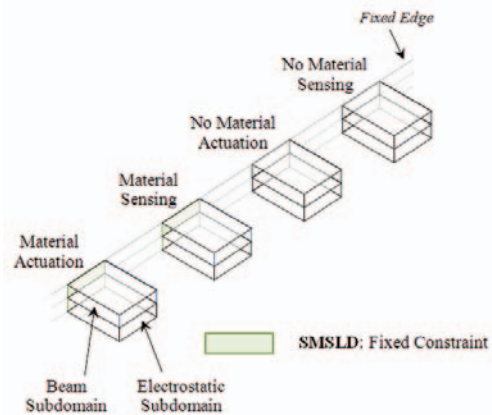|	**Beam Subdomains**	**Electrostatic Subdomains**
Material+Actuation **or** *Material+Sensing*		
SMSLD	Active/Poly-Si	Inactive
No Material+Actuation **or** *No Material+Sensing*		
SMSLD	Inactive	Inactive

Figure 4: Boundary settings for the natural frequency computation of the device before and after mass accumulation on the sensor

The boundary settings for this analysis are illustrated in Figure 4. The sketch illustrates boundary assignments for each type of subdomain configuration along the fixed edge. Those regions not along the fixed edge maintain the same boundary conditions with the exception of the fixed constraint in the SMSLD application. The boundaries along the fixed edge of the beam subdomains with material were assigned a fixed constraint. The remaining boundaries of the beam subdomains with material maintained a free boundary condition.

4.3 Model 2: Stationary Analysis

Subsequent to the natural frequency computations (Section 4.2), a coupled, stationary analysis for the static deflection of the beam was performed for the assigned actuation voltage (Step 2c in Figure 2). This model utilized the SMSLD, ALE and EMES applications [2]. A function was created in MATLAB to compute the indices for proper assignment of subdomain and boundary properties in each application.

Table II summarizes the subdomain settings used in this model for each application. Beam subdomains with material were active in the SMSLD application with the material properties of poly-silicon, assigned a mesh deformation in the ALE application consistent with the physics from the output of the SMSLD application, and inactive in the EMES application. The remaining subdomains were inactive in the SMSLD

Table II: Subdomain settings for the static deflection analysis of the sensor under an electrostatic load

	Beam Subdomains	Electrostatic Subdomains
Material+Actuation **or** *Material+Sensing*		
SMSLD	Active/Poly-Si	Inactive
ALE	Active/Physics Induced Deform.	Active/Free Deform.
EMES	Inactive	Active/Air
No Material+Actuation **or** *No Material+Sensing*		
SMSLD	Inactive	Inactive
ALE	Active/Free Deform.	Active/Free Deform.
EMES	Active/Air	Active/Air

Figure 5: Boundary settings for the static deflection analysis of the sensor under an electrostatic load

application, allowed free mesh deformation in the ALE application and active with the material properties of air in the EMES application.

The boundary settings for this analysis are illustrated in Figure 5. The sketch illustrates boundary assignments for each type of subdomain configuration along the fixed edge. Those regions not along the fixed edge maintained the same boundary conditions with the exception of the fixed constraint in the SMSLD application and the fixed mesh in the ALE application.

In the SMSLD application, a fixed constraint was applied to boundaries of beam subdomains with material along the fixed edge. The bottom surfaces of all beam subdomains with material were assigned a boundary load. The load assigned was the electrostatic force computed in the EMES application.

In the ALE application, only boundaries corresponding to beam subdomains with material were assigned a mesh deformation consistent with the output of the SMSLD application. Boundaries of all subdomains along the fixed edge, bottom surfaces of electrostatic domains, and all boundaries defined by the encompassing 3D block (referred to in Section 4.1, but not shown in Figure 5) were prescribed zero mesh deformation.

In the EMES application, the bottom surfaces of beam subdomains were assigned an electric potential. The bottom surfaces of electrostatic subdomains were assigned a ground condition if part of an actuation configuration and a zero charge condition if part of a sensing configuration.
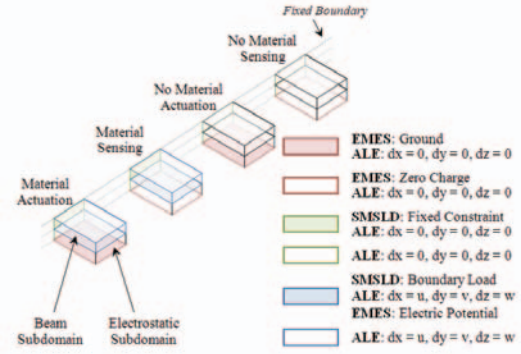
Electrostatic MEMS are subject to an instability called "pull-down" at approximately one-third of the initial gap for a rectangular shaped cantilever for which the actuation electrode is directly below the tip of the beam [3]. "Pull-down" causes the beam to snap down and make contact with the lower electrode. For this application, this is not a desirable situation and can potentially cause damage to the device. Therefore, a "pull-down" check was created that detected a COMSOL generated warning suggesting the solution has not converged, since there is a numerical challenge with computing a fully-coupled solution with displacements exceeding "pull-down." Any configuration that experiences "pull-down" in the static deflection analysis is considered undesirable and assigned a high fitness value.

4.4 Model 3: Frequency Response Analysis

An accumulated change in mass will ultimately affect the frequency response of the sensor. Therefore, a frequency response analysis in COMSOL using the SMSLD and MMFD application was performed next (Step 2e in Figure 2). The frequency response analysis in COMSOL allows for the computation of the steady-state amplitude of the device when actuated at a single frequency. The model evaluated the sensor before and after mass accumulation, at both frequencies computed by Model 1 (Section 4.2), for a total of 4 solutions. A function was created in MATLAB to compute the indices for proper assignment of subdomain and boundary properties.

Table III: Subdomain settings for the frequency response analysis of the device before and after mass accumulation on the sensor

	Beam Subdomains	Electrostatic Subdomains
Material+Actuation **or** *Material+Sensing*		
SMSLD	Active/Poly-Si	Inactive
	Initial Displacement	-
No Material+Actuation **or** *No Material+Sensing*		
SMSLD	Inactive	Inactive

Table III summarizes the subdomain settings used in this model for each application. The subdomain settings are similar to the settings in Model 1 (Section 4.2); however the beam subdomains are assigned an initial displacement according to the static deflection computed in Model 2 (Section 4.3). The MMFD is strictly a boundary application and does not require subdomain settings.

The boundary settings for Model 3 are illustrated in Figure 6. Again, the sketch illustrates boundary assignments for each type of subdomain configuration along the fixed edge. Those regions not along the fixed edge maintained the same boundary conditions with the exception of the fixed constraint in the SMSLD application.

In the SMSLD application, a fixed constraint was applied to boundaries of beam subdomains with material along the fixed edge. The bottom surfaces of all beam subdomains with material were assigned a boundary load.
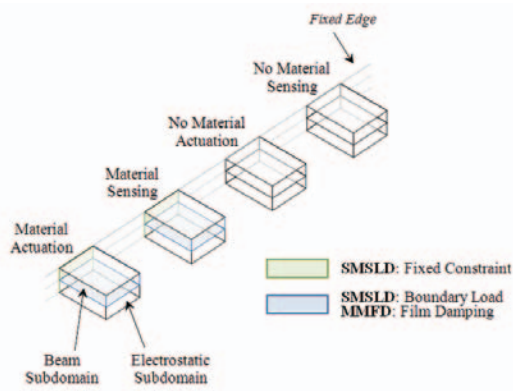

Figure 6: Boundary settings for the frequency response analysis computation of the device before and after mass accumulation on the sensor

The load assigned was the squeezed-film damping force computed in the MMFD application.

In the MMFD application, all bottom surfaces of beam subdomains with material were assigned a film damping boundary. The surrounding air pressure was assigned to atmospheric and the initial gap was defined individually according to each configuration (Section 2, Figure 1).

4.5 Fitness Evaluation

Under zero actuation, the device will output a nominal capacitance, c, that is dependent on the initial gap and can be estimated, as shown in Eq (1), according to the capacitance for two parallel plates [3], given the area of the plates, A, permittivity of free space, ε, and the initial gap, g_0. Other analytical capacitance models that take into account fringing forces of the electrostatic field for devices of defined geometric families are given in [4-6].

$$\text{Eq (1)} \quad C = \frac{\varepsilon A}{g_0}$$

When actuated at a single frequency, at steady-state the device will output a measurable amplitude change in capacitance, dependent upon the deflection. In Model 3 (Section 4.4), the steady-state change in amplitude, w, of the bottom surfaces of beam subdomains assigned material and denoted as sensing, was integrated and averaged over the entire sensing electrode area, A_{sensed}, to compute the magnitude steady-state sensed capacitance, C_{sensed}, shown in Eq (2).

$$\text{Eq (2)} \quad C_{sensed} = \frac{\varepsilon A_{sensed}}{\left(\frac{\int w dA}{A_{sensed}} \right)}$$

By subtracting the magnitude of the sensed capacitance of the sensor before and after mass accumulation, the change in sensed capacitance for that configuration was determined for the actuation frequency, $\Delta C_{sensedf1}$, as shown in Eq (3).

$$\text{Eq (3)} \quad \Delta C_{sensed f1} = \left| C_{sensed_{beam+mass}} - C_{sensed_{beam}} \right|$$

Since the analysis is completed for two frequencies, a 2-point RMS computation was used. The genetic algorithm aimed to minimize the fitness through the generations, thus the fitness value, *FV*, for each configuration was the negative value of the 2-point RMS average sensed change in capacitance, shown in Eq (4).

$$\text{Eq (4)} \quad FV = -\sqrt{{\Delta C_{sensed_{f1}}}^2 + {\Delta C_{sensed_{f2}}}^2}$$

5. Results and Future Work

A sample run of the design tool was run to show the improvement in design (i.e. reduction in fitness). Increasing the population size or the number of generations increases the number of configurations evaluated and improves the probability of fitness reduction at the cost of solution time. A population of 100 members was chosen and the tool ran for 15 generations. The output design was the configuration described in Figure 1. Through the generations the fitness was reduced by a factor of 10. The best fitness value and the average fitness value for each generation are illustrated in Figure 7.

Future work is focusing on improving the computational efficiency of the design tool. An analytical electrostatic model will be developed to eliminate the need for the deformed mesh and electrostatic applications, but still take into account the possible fringing effects of the configurations that can be generated by the unique material and electrode distributions for modeling of both sensing and actuation. Improved efficiency will make the automated design tool far more practical.
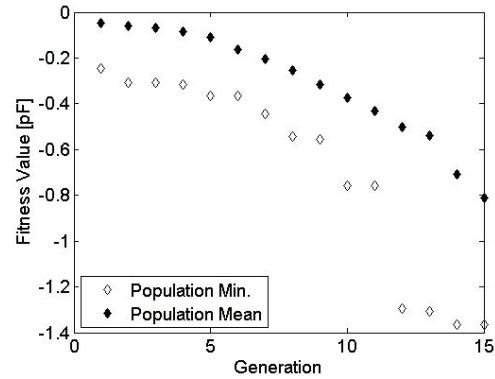

Figure 7: Average and best fitness values for each generation in the automated design process that led to the device configuration described in Figure 1.

5. References

1. Raulli, M. and Maute, K., Topology Optimization of Electrostatic MEMS, *AIAA/ISSMO Multidisciplinary Analysis and Optimization Conference*, Albany, NY (2004)
2. Comsol Multiphysics, *MEMS Module: Model Library*, Ver. 3.3 pp. 8-26 (2006)
3. Elata, D., *MEMS/NEMS Handbook: Techniques & Applications*, (4) "Modeling the Electromechanical Response of Electrostatic Actuators", pp. 1085-1111 (2006)
4. Palmer, H.B., The Capacitance of a Parallel-Plate Capacitor by the Schwartz-Christoffel Transformation, *Transactions on AIEE*, Vol. **56**, No. **3**, pp. 363-366 (1937)
5. Elliott, R.S., *Electromagnetics*, pp. 187-188, McGraw-Hill, Inc, New York, NY (1966)
6. Yuan, C.P. and Trick, T.N., A Simple Formula for the Estimation of the Capacitance of Two-Dimensional Interconnects in VLSI Circuits, *IEEE Electron Device Letters*, Vol. **EDL-3**, No. **12**, pp. 391-393 (1982)

9. Acknowledgements